Broadband coherent anti-Stokes Raman scattering in silicon

Prakash Koonath, Daniel R. Solli, and Bahram Jalali*

Department of Electrical Engineering, University of California–Los Angeles, Los Angeles, California 90095-1594, USA
**Corresponding author: jalali@ucla.edu*

Received September 28, 2009; revised December 1, 2009; accepted December 7, 2009; posted December 23, 2009 (Doc. ID 117846); published January 26, 2010

In silicon devices, the spectral bandwidth of coherent anti-Stokes Raman scattering (CARS) is limited by the narrowband nature of the Raman process in this medium. In this Letter, we report the observation of broadband wavelength conversion in silicon through CARS enhanced by the self-phase-modulation-induced spectral broadening of the optical pump. The CARS conversion over a bandwidth substantially greater than the intrinsic Raman linewidth is demonstrated yielding conversion efficiencies as high as 1%. Numerical simulations are performed to explain the spectral features observed in the spectrum of the anti-Stokes signal.

OCIS codes: 300.6230, 250.4390, 190.5890, 130.3120.

Wavelength conversion offers a means to transfer optical energy from a given wavelength to a preferred part of the spectrum where the processing of the information is optimal. It finds application in WDM systems, for example, in the addition or dropping of information channels, in optical switching systems and other signal processing architectures [1–3]. Coherent anti-Stokes Raman scattering (CARS) has been demonstrated in silicon as a way of obtaining an efficient wavelength conversion at telecommunication wavelengths [4,5]. The nonlinear Raman susceptibility of silicon transfers energy from a Stokes field that is 15.6 THz downshifted from the pump wavelength to an anti-Stokes field, 15.6 THz upshifted from the pump signal, through a resonant four-wave mixing (FWM) process. This is depicted schematically in Fig. 1.

CARS produces a more efficient wavelength conversion than that obtained by electronic (broadband) FWM, as the resonant Raman susceptibility is much stronger than its electronic counterpart [4]. On the other hand, this resonance, which leads to a Lorentzian profile with a bandwidth of around 105 GHz in silicon, limits the spectral bandwidth over which efficient wavelength conversion may be achieved. Although pump lasers at multiple wavelengths can be used to broaden the bandwidth of wavelength conversion, this strategy adds to the cost, power consumption, and complexity of the chip-scale coupling architecture. In this Letter, we utilize a simple design to demonstrate the CARS conversion in silicon over a spectral range, much broader than the intrinsic linewidth of the Raman process, while achieving conversion efficiencies of ~1%. These achievements are realized by utilizing a pulsed pump source that is modified by self-phase modulation (SPM) within the silicon medium; this nonlinear effect broadens the input pulse inside the device during propagation.

It should be noted that the phase matching between the pump, Stokes, and the anti-Stokes fields also influences the efficiency of the wavelength conversion as in any FWM process. Recent work has demonstrated that phase matching can be achieved in silicon waveguides with waveguide dispersion engineering permitting an efficient broadband wavelength conversion via electronic FWM [6]. On the other hand, appreciable conversion efficiencies can also be obtained in the absence of phase matching by employing an intense pump wave; in this situation, the conversion efficiency increases substantially and becomes less sensitive to phase mismatch [5]. The present results are achieved without phase matching using a waveguide whose dispersive properties are essentially those of bulk silicon.

The intense optical pulses propagating through a nonlinear medium like silicon modulate the refractive index of the medium. As a result, a pulse produces a dynamic modulation of its own phase (SPM), which broadens its spectrum. In silicon, the SPM has two contributions: (1) Kerr nonlinearity and (2) free-carrier refraction (FCR), the modulation of the refractive index caused by the carriers generated during two-photon absorption (TPA). The combined effect of these two effects produces a blueshifted broadened spectrum, the details of which have been discussed elsewhere [7]. When this spectrally broadened pulse copropagates with a Stokes signal, it acts as a broadband Raman pump generating a CARS conversion over a bandwidth that is wider than that of the natural linewidth of silicon. The Stokes signal also undergoes Raman amplification during the process.

In our experiments, picosecond optical pulses (~2 ps) from a mode-locked laser operating at 1550 nm are split to produce pump and probe pulses. One portion is stretched, amplified, and compressed to

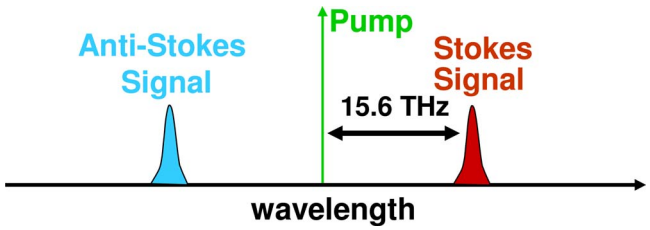

Fig. 1. (Color online) Schematic depiction of wavelength conversion through CARS silicon.

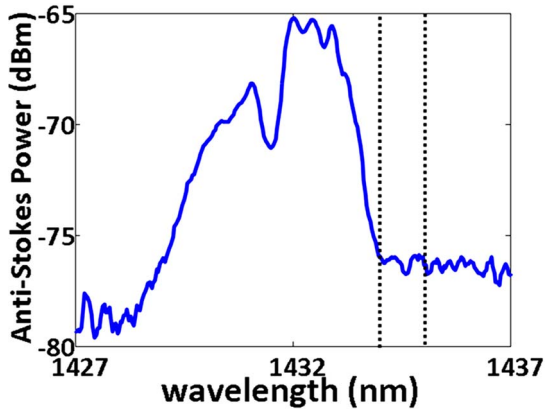

Fig. 2. (Color online) Measured spectrum of broadband CARS conversion in silicon. The 3 dB bandwidth of the Raman process for a pump wavelength at 1550 nm is delineated by vertical dotted lines for the purpose of comparison.

generate ~40 ps pump pulses with a peak power of 230 W. The other portion is amplified and sent through a nonlinear fiber to generate a flat optical continuum centered at the Stokes wavelength (~1685 nm). The pump and Stokes pulses are synchronized via an optical delay line, combined in free space, and coupled to a silicon waveguide (2 cm length; mode area ~2.8 μm^2). The input coupling loss of the setup is estimated to be approximately 6.6 dB, and the waveguide has a linear propagation loss of ~0.5 dB/cm. At the output of the waveguide, light is collected and fed to an optical spectrum analyzer (OSA).

The measured spectrum of the broadband CARS wavelength conversion is shown in Fig. 2. The power level of the input Stokes signal was around −45 dBm, which translates to a conversion efficiency of ~1% (ratio of the output anti-Stokes power to the coupled Stokes power) at the peak of the anti-Stokes signal. As shown in Fig. 2, conversion efficiencies of 0.3% are obtained in a semiconductor medium over more than three times the intrinsic Raman linewidth. Both the SPM broadening of the pump as well as its initial linewidth contribute to the observed CARS bandwidth. Typically stimulated linewidths are narrower than expected from the input pump bandwidth and intrinsic Raman linewidth, yet here the SPM causes the CARS linewidth to be broader than the input width. We also note that achieving a broadened CARS spectrum reduces the absolute conversion efficiency as we have obtained significantly higher efficiencies when using pump intensities that do not broaden the pump. However, even in the broadened case, the conversion efficiencies reported here are 2 orders of magnitude larger than any previously reported values for CARS using cw signals. We also expect that this broadband CARS conversion efficiency can be substantially improved by phase matching with waveguide dispersion engineering.

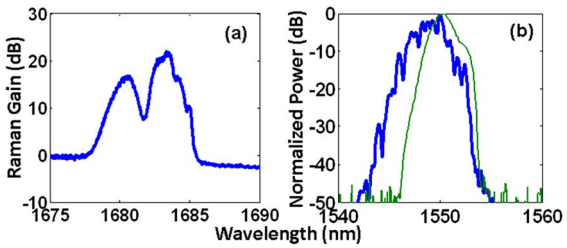

Fig. 3. (Color online) (a) Measured spectrum of the Raman gain at the Stokes wavelength, (b) the optical pump at 1550 nm. The dotted curve in (b) delineates the spectrum of the input pump signal. The broadening and the blueshift are noticeable in both the pump as well as the Raman gain.

The center wavelength of the broadened CARS spectrum is clearly blueshifted relative to the natural anti-Stokes position for a 1550 nm pump. This shift arises because of the effect of the SPM on the pump: the broadened spectrum of the pump wave in Fig. 3(b) is also blueshifted. For a pump wavelength at 1550 nm, the expected center wavelength of the anti-Stokes field in silicon is ~1434.4 nm and that of the Stokes field is ~1685.9 nm. The blueshift of the pump [Fig. 3(b)] wave also influences the amplified Stokes signal shown in Fig. 3(a). As reported previously [8], the Stokes signal exhibits a broadband gain akin to the broadband CARS conversion seen in the anti-Stokes signal. The on–off Raman gain, here as high as 20 dB, further facilitates the CARS efficiency. The evolution of the pump spectrum and the generation of the CARS signal take place in concert along the waveguide. Therefore, the output CARS spectrum represents the cumulative interplay of these processes rather than simply replicating the pump spectrum. Furthermore, the convolution of the pump spectrum with the linewidth of the Raman response smears out many of the fine spectral features.

We also study the CARS wavelength conversion numerically by simultaneously solving the nonlinear Schrödinger equation and the differential equation that describes the evolution of free-carriers, which do not decay on the time scale of a single pulse but disappear prior to the next pulse. The complete prescription for this numerical analysis has been discussed in detail elsewhere [8,9]. Pump pulses of 230 W peak power and width ~40 ps (1.8 nm bandwidth) copropagate with broadband, chirped (2 ps duration) probe pulses covering the Stokes wavelength. The simulated spectra of broadband CARS conversion and Raman gain are shown in Fig. 4 for a relative delay of 10 ps between the pump and the Stokes pulses (Stokes pulse timed at the pump's leading edge). There is qualitative agreement on the spectral features of the simulated and experimentally measured spectra. It is seen from the simulations that the relative delay between the pump and the Stokes pulse strongly influences the spectral characteristics and the CARS conversion efficiency, as we also observed experimentally. Figure 5 plots the numerical spectra for three different values of relative delay illustrating the effect of this parameter. This impact of the relative delay may be understood by considering the following: (1) the evolution of the temporal profile of the pump as it propagates through the waveguide and (2) the distribution of the frequencies generated by the SPM underneath the pump envelope (i.e., the chirp of the pump). The temporal profile and the cumulative chirp of the pump pulse (the chirp that has been ac-

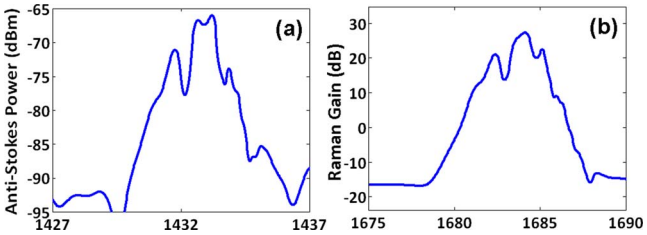

Fig. 4. (Color online) Simulated spectra of (a) anti-Stokes signal and (b) Stokes signal. These spectra correspond to a delay of 10 ps between the pump and the broadband Stokes signal with the Stokes signal timed at the leading edge of the pump.

cumulated by the pump pulse for a given propagation distance) are shown in Fig. 6 for various points along the waveguide (the arrow represents the direction of increasing distance into the waveguide). The pump gets depleted by TPA and free-carrier absorption (FCA), as seen from Fig. 6(a), becoming asymmetric as its peak shifts toward the leading edge of the pulse. This shift of the peak is primarily due to the cumulative nature of the FCA dynamics, which becomes stronger toward the trailing edge of the pulse. In a similar fashion, the peak of the cumulative chirp of the pulse also shifts toward the leading edge of the pulse. Most of the chirp is positive (blueshift) indicating the dominance of FCR in the SPM process and also accounting for the blueshift observed both experimentally and numerically in the CARS and the Raman gain spectra. The small redshift seen near the leading edge of the pulse is caused by the Kerr effect, which is strongest close to the steepest part of the pulse. Since the broadening of the CARS spectrum relies on the new frequency components created by the SPM, it is desirable to temporally collocate the Stokes pulse where most of these components are generated. Furthermore, the pulse becomes progressively asymmetric as it propagates inside the waveguide shifting its peak value toward earlier times. For most of the propagation, the peak of the pulse lies in the range 10–25 ps earlier than the initial pulse. This also makes it beneficial to have the

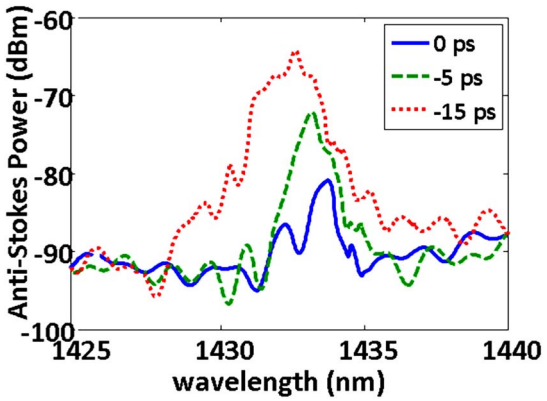

Fig. 5. (Color online) Simulated anti-Stokes signal for different values of delay between the pump and the broadband input Stokes pulses.

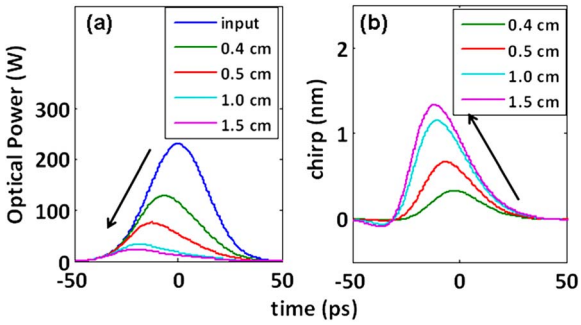

Fig. 6. (Color online) Impact of free-carrier nonlinearities obtained through simulations on (a) the temporal profile of the pump pulse and (b) the chirp of the pump pulse. The relatively minor influence of the Kerr effect on chirp is seen at the leading edge of the pulse in (b). (b) is corrected for the chirp of the pump pulse at the input.

Stokes pulse timed on the leading edge of the pump pulse to observe an efficient CARS conversion. The timing between the pump and Stokes pulses thus provides a way to control the CARS profile. Since the SPM depends strongly on the pump power, it is clear that the profile may be controlled by varying this parameter as well.

In conclusion, we report the observation of an efficient CARS conversion in silicon over a broad spectral bandwidth. This is achieved utilizing the simultaneous broadening of the pump by the SPM during the CARS conversion process. The dynamics of the CARS conversion process is also studied by numerically solving the propagation of the pump, Stokes, and anti-Stokes pulses in the silicon medium. A good agreement is observed between the experimentally obtained results and the simulated spectra with the spectral characteristics significantly affected by the dynamics of the free-carrier generation. Since these dynamics depend on the pulse characteristics (pump power, timing, etc.), the spectrum of the CARS conversion can be tailored by tuning these parameters.

References

1. J. M. Tang, P. S. Spencer, and K. A. Shore, Appl. Phys. Lett. **75**, 2710 (1999).
2. T. Sylvestre, A. Kudlinski, A. Mussot, J. F. Gleyze, A. Jolly, and H. Maillotte, Appl. Phys. Lett. **94**, 111104 (2009).
3. R. Espinola, J. Dadap, R. Osgood, Jr., S. McNab, and Y. Vlasov, Opt. Express **13**, 4341 (2005).
4. V. Raghunathan, R. Claps, D. Dimitropoulos, and B. Jalali, Appl. Phys. Lett. **85**, 34 (2004).
5. P. Koonath, D. R. Solli, and B. Jalali, in *Conference on Lasers and Electro-Optics* (Optical Society of America, 2008), paper CThE3.
6. M. A. Foster, A. C. Turner, J. E. Sharping, B. S. Schmidt, M. Lipson, and A. L. Gaeta, Nature **441**, 960 (2006).
7. P. Koonath, D. R. Solli, and B. Jalali, Appl. Phys. Lett. **93**, 091114 (2008).
8. D. R. Solli, P. Koonath, and B. Jalali, Appl. Phys. Lett. **93**, 191105 (2008).
9. Q. Lin, O. J. Painter, and G. P. Agrawal, Opt. Express **15**, 16604 (2007).